

1 **Effects of anthropogenic activities on the molecular composition of urban**
2 **organic aerosols: an ultrahigh resolution mass spectrometry study**

3
4 I. Kourtchev¹, I.P. O'Connor², C. Giorio¹, S. Fuller¹, K. Kristenen³, W. Maenhaut^{4,5}, J.C.
5 Wenger², J.R. Sodeau², M. Glasius³, and M.Kalberer¹

6
7
8 ¹Department of Chemistry, University of Cambridge, Cambridge, CB2 1EW, UK

9 ²Department of Chemistry and Environmental Research Institute, University College Cork,
10 Cork, Ireland

11 ³Department of Chemistry, Aarhus University, Aarhus, DK-8000, Denmark

12 ⁴Department of Analytical Chemistry, Ghent University, Krijgslaan 281, S12, BE-9000
13 Ghent, Belgium

14 ⁵Department of Pharmaceutical Sciences, University of Antwerp, Universiteitsplein 1, BE-
15 2610 Antwerp, Belgium

16
17
18 *Corresponding authors: ink22@cam.ac.uk

19
20
21
22
23
24

25 **Abstract**

26 The identification of the organic composition of atmospheric aerosols is necessary to develop
27 effective air pollution mitigation strategies. However, the majority of the organic aerosol
28 mass is poorly characterized and its detailed analysis is a major analytical challenge. In this
29 study, we applied state-of-the-art direct infusion nano-electrospray (nanoESI) ultrahigh
30 resolution mass spectrometry (UHR-MS) and liquid chromatography ESI Quadrupole Time-
31 of-Flight (Q-TOF) MS for the analysis of the organic fraction of fine particulate matter
32 (PM_{2.5}) from an urban location in Cork, Ireland. Comprehensive mass spectral data
33 evaluation approaches (e.g., Kendrick Mass Defect and Van Krevelen) were used to identify
34 compound classes and mass distributions of the detected species. Up to 850 elemental
35 formulae were identified in negative mode nanoESI-UHR-MS. Nitrogen and/or sulfur
36 containing organic species contributed up to 40% of the total identified formulae and
37 exhibited strong diurnal variations suggesting the importance of night-time NO₃ chemistry at
38 the site. The presence of a large number of oxidised aromatic and nitroaromatic compounds
39 in the samples indicated a strong anthropogenic influence, i.e., from traffic emissions and
40 burning of domestic solid fuel (DSF) material. Most of the identified biogenic secondary
41 organic aerosol (SOA) compounds were later-generation nitrogen- and sulfur -containing
42 products, indicating that SOA composition is strongly affected by anthropogenic oxidants
43 such as NO_x and SO₂. Unsaturated and saturated C₁₂-C₂₀ fatty acids were found to be most
44 abundant homologs with composition reflecting primary marine origin. The results of this
45 work demonstrate that the studied site is a very complex environment affected by a variety of
46 anthropogenic activities and natural sources.

47
48
49

50 **Introduction**

51 Particulate matter (PM), also referred as atmospheric aerosols, is linked to air quality and
52 climate. A significant fraction of PM is associated with organic carbon (OC) which can
53 contribute up to 90% of the total aerosol mass in certain locations (Kanakidou et al., 2005).
54 Organic aerosols can either be emitted directly (primary organic aerosol, POA) or formed
55 through gas-to-particle conversion processes or oxidation of volatile organic compounds
56 (VOCs) within the atmosphere (secondary organic aerosol, SOA). Various sources contribute
57 to formation of PM and include anthropogenic sources such as use of diesel and petrol,
58 burning of fossil fuel and biomass. Biogenic sources include VOCs emitted by vegetation.
59 Urban environments provide very unique systems where both anthropogenic and biogenic
60 emissions coexist resulting in the formation of extremely complex OA. For example,
61 anthropogenic oxides of nitrogen (NO_x) are shown to react with a range of BVOCs causing
62 high regional ozone concentrations (Chameides et al., 1988) as well as being responsible for
63 formation of organonitrates, ON (e.g., Roberts, 1990; Day et al., 2010) and nitrooxy-
64 organosulphates, NOS (Surratt et al., 2008) that are important SOA components.

65 The identification of organic composition of aerosols remains a major analytical challenge
66 which results in a poor understanding of aerosol sources. But only a comprehensive
67 knowledge of aerosol sources allows developing effective air pollution mitigation strategies.
68 Considering that OA composed of thousands of organic compounds, which cover a wide
69 range of polarities, volatilities and masses (Goldstein and Galbally, 2007), it is difficult to
70 find a single analytical technique for their detailed chemical analysis at the molecular level.
71 Conventional analytical methods based on gas chromatography (GC) and liquid
72 chromatography (LC) mass spectrometry are very effective in the identification of specific
73 marker compounds for certain aerosol sources such as biomass burning, vehicular and
74 cooking contributions. However, these methods are not capable of resolving the highly
75 complex mixtures with a wide variety of physico-chemical properties leading to a very large
76 fraction of OC being unidentified. In a previous study at Cork harbour, Ireland, conducted
77 during summer 2008 the detected marker compounds that are characteristic for domestic solid
78 fuel burning, fungal spores and oxidation of isoprene and α - and β -pinene could only explain
79 20% of the OC (Kourtchev et al., 2011). Moreover, commonly used mass spectrometers,
80 which are often used as detectors following chromatographic separation, do not have
81 sufficient mass-resolving power to distinguish and differentiate all compounds present in the
82 complex mixture of organic aerosol. Ultrahigh resolution mass spectrometry (UHRMS)
83 methods have shown a great potential in solving this longstanding problem. UHRMS (i.e.,

84 Fourier transform ion cyclotron resonance MS and Orbitrap MS) have a mass resolution
85 power that is at least one order of magnitude higher (~100 000) than conventional MS and
86 thus, when coupled with soft ionisation techniques, can provide a detailed molecular
87 composition of organic aerosol (Nizkorodov et al., 2011). Nano-electrospray (nanoESI)
88 ionisation is a promising soft ionisation technique for the analysis of OA due to its high
89 sensitivity toward a variety of analytes and low sample volume requirements (less than 5 μ L
90 are required for nanoESI analysis compared to at least 100 μ L required by conventional ESI
91 sources). In a direct infusion analysis of complex organic mixtures with conventional ESI
92 sources the competition for ion formation, i.e., matrix effects, is one of the primary problems.
93 The significantly lower flow rates employed by nanoESI decrease the droplet size and
94 increase the charge concentration on the droplet resulting in less competition for ion
95 formation and lower ion suppression (Love et al., 2011).

96 The objective of the current study is to apply nanoESI UHRMS to determine the molecular
97 composition of urban PM_{2.5} (particles with $\leq 2.5\mu\text{m}$). Aerosol samples were collected at the
98 industrial site in Cork Ireland during summer with the aim to obtain aerosol particles of
99 mixed biogenic and anthropogenic origin. Considering that direct infusion analysis is a
100 qualitative technique, aerosol samples were additionally analysed by LC - ESI Quadrupole
101 Time-of-Flight (Q-TOF) MS for the NOS and organosulphates (OS) that reflect emissions
102 from mixed sources. The results clearly demonstrate that the overall composition of OA is
103 dominated by anthropogenic sources such as traffic and biomass burning and that the
104 biogenic OA is significantly affected by anthropogenic oxidants (e.g., NO_x and SO₂).

105

106 **Methodology**

107 *Ambient samples*

108 Aerosol samples were collected at the Industrial Estate and Docks, Cork, Ireland (51°54'5 N,
109 8°24'38 W). A detailed description of the site is given elsewhere (Healy et al., 2010;
110 Kourtchev et al., 2011). Briefly, the site is located approximately 3 km east of Cork city
111 centre with a population of about 120,000. The site is located near a shipping berth, a main
112 road and residential areas. The vegetation that surrounds the site manly consists of shrubs and
113 native deciduous trees.

114 PM_{2.5} aerosol samples were collected on quartz fiber filters (Pallflex Tissuquartz 2500QAT-
115 UP, 150 mm diameter, preheated for 24 h at 650°C) using a High Volume (Digitel DHA-80,
116 Switzerland) sampler with a flow rate of 500 L min⁻¹. In total 14 samples were collected
117 during 3-19 September 2011. Considering relatively wet and cloudy weather prevailing

118 during the sampling period only five separate day and night samples were collected during 3-
119 6 September, 2011. The remaining samples were collected at 24 hour (6 - 11 September,
120 2011) and 48 hour resolution (11 - 19 September, 2011) to enable sufficient collection of
121 aerosol mass required for LC/MS analysis. The corresponding sampling collection time and
122 dates are shown in Table S1.

123

124 *Aerosol sample analysis*

125 All ambient filters were analysed for organic carbon (OC) and elemental carbon (EC) using a
126 thermal-optical transmission (TOT) technique (Birch and Cary, 1996).

127 For the UHRMS analysis, aerosol samples were extracted as described elsewhere (Kourtchev
128 et al., 2013a). For each sample, a part of the quartz fibre filter (6–30 cm²), depending on OC
129 or total aerosol loading, was extracted three times with 5 mL of methanol (Optima® grade,
130 Fisher Scientific) under ultrasonic agitation for 30 min in ice cold water. The three extracts
131 were combined, filtered through a 0.2 μm ISO-Disc™ PTFE filter (Supelco, Bellefonte, PA,
132 USA) and reduced by volume to approximately 200 μL under a gentle stream of nitrogen.
133 The final extracts were analysed using an ultrahigh resolution LTQ Orbitrap Velos mass
134 spectrometer (Thermo Fisher, Bremen, Germany) equipped with a TriVersa Nanomate
135 robotic nanoflow chip-based ESI source (Advion Biosciences, Ithaca NY, USA). The
136 Orbitrap MS instrument calibration, settings and mass spectral data interpretation are
137 described in the Supporting Information (SI). Double bond equivalent (DBE) for each
138 individual formula was calculated using Xcalibur 2.1 (Thermo Fisher Scientific, USA)
139 software. All molar ratios, DBE factors and chemical formulae presented in this paper refer to
140 neutral molecules.

141 For LC/MS analysis, a part (20 cm²) of the filter was spiked with internal recovery standard
142 (0.6 μg camphorsulfonic acid). Aerosol samples were extracted in acetonitrile (grade) in a
143 cooled ultrasonic bath for 20 minutes. Extracts were evaporated to dryness and reconstituted
144 in 200 μL of 0.1 % acetic acid and 3 % acetonitrile in water. Sample extracts were analysed
145 using a Dionex Ultimate 3000 HPLC system coupled through an ESI inlet to a Q-TOF mass
146 spectrometer (microTOFq) (Bruker Daltonics GmbH, Bremen, Germany). The ESI-QTOF
147 operating conditions are detailed in the SI.

148

149 *Meteorological data*

150 The meteorological data was obtained from the Cork Airport monitoring station. During the
151 sampling period the wind was predominantly from west-southwesterly direction (Fig 1). The

152 period was accompanied by light/gentle (wind speed $>2 \text{ m s}^{-2}$) and strong wind ($>6 \text{ m s}^{-2}$)
153 (Fig 1c) with the exception of two episodes corresponding to samples from 3 September and
154 13-15 September, which were characterised by very calm wind conditions ($\leq 2 \text{ m s}^{-2}$) (Fig 1a
155 and b).

156 The average air temperature and relative humidity were $12.5 \pm 2.0 \text{ }^{\circ}\text{C}$ and $90.2 \pm 9.5\%$,
157 respectively. The whole sampling period, with exception of 3 September and 13-15
158 September 2011, was accompanied by at least light precipitation.

159

160 **Results and discussion**

161 High resolution nanoESI mass spectra of a day- and night- sample collected on 3 September
162 and 4 September respectively are shown in Fig. 2. Throughout the sampling period very high
163 variability between the molecular compositions was observed; however, despite this, all mass
164 spectra appear to be mainly composed of compounds with molecular weight (MW) below
165 400Da. Although ions above 400 Da were observed in all samples up to the measured 650 Da
166 range, their maximum contribution to the total number of formulae was less than 7%. The
167 majorities of the ions with masses above 300 Da were nitrogen and/or sulfur containing
168 species or oxidised aromatic compounds as described below. Depending on the sample, 271-
169 849 elemental formulae were identified and included four subgroups: CHO, CHOS, CHON
170 and CHONS. CHO was the most abundant subgroup in all samples (average $59.4 \pm 3.9\%$ of
171 the total formulae), followed by CHON ($21.8 \pm 3.6\%$), CHOS ($13.5 \pm 3.6\%$), and CHONS
172 ($5.2 \pm 2.4\%$). The highest number of molecular formulae (up to about 850) was observed
173 during 3 September, when the wind speed fell below 2 m s^{-1} (Fig. 1a). Higher wind speeds
174 were generally associated with greater dilution of aerosol as a larger volume of air passes
175 over local emission sources.

176 Although only 5 out of 14 samples were collected during separate day and night periods, we
177 could clearly observe an increase in the ratio of molecular formulae containing CHON and
178 CHONS to the total number of peaks in night time samples (average 16% and 8%,
179 respectively) compared to the day time samples. This difference is also apparent in the mass
180 spectra shown in Figure 2. Generally, ON are formed in polluted air during the day through
181 reaction with NO and at night through NO_3 radical-initiated reactions with alkenes (Day et
182 al., 2010). The increased ratio of ON molecules during the night might indicate the
183 importance of NO_3 chemistry at the sampling site or more pronounced partitioning into the
184 particle phase. Similar diurnal trend for nitrogen containing compounds was observed for the
185 aerosol samples collected at Bakersfield, USA (O'Brien et al., 2013). It should be noted,

186 however, that a significantly higher fraction of nitrogen containing compounds (up to 53%,
187 by number) was observed in the latter study. The differences could be related to specific
188 emissions of gas phase ammonia at the Bakersfield site, which is a region known for
189 substantial agricultural livestock emissions. In this respect, O'Brien et al. (2013) suggested
190 that about 50% of their nitrogen containing organic compounds could have been formed
191 through reactions of gaseous ammonia with SOA components. The increased fraction of OS
192 during the night in the Cork samples could be explained by enhanced gas-to-particle
193 partitioning at the cooler night-time temperatures. It has been suggested that some of the
194 volatile species (e.g., pinanediol nitrates) need cooler temperatures to partition to the particle
195 phase where they are subsequently sulphated (e.g., Surratt et al., 2008).

196 The average elemental ratios for molecules containing CHO compared to the total
197 number of formulas showed rather low variation throughout the sampling period with
198 0.39 ± 0.04 and 1.28 ± 0.09 (mean value \pm standard deviation) for O/C and H/C, respectively.
199 These values are comparable to average O/C obtained using UHRMS from mixed urban-rural
200 aerosol from Bakersfield, USA: 0.33 and 0.37 during a day and night, respectively (O'Brien
201 et al., 2013). However, higher values were reported for urban aerosol from Cambridge, UK:
202 0.55-0.6 (Rincón et al., 2012) and boreal forest aerosol from Hyytiälä, Finland: 0.52
203 (Kourtchev et al., 2013a). Generally, higher O/C values are given for SOA generated in
204 laboratory experiments from BVOCs, e.g., α -pinene, 0.42-0.55 (Putman et al., 2012),
205 limonene, 0.5-0.6 (Kundu et al., 2012), photo-oxidation of isoprene under low-NO_x
206 conditions, 0.54 (Nguyen et al., 2011) and BVOC mixture containing α -, β -pinene, Δ_3 -carene
207 and isoprene, 0.58 (Kourtchev et al., 2013b).

208

209 *Oxidised aromatics*

210 The Van Krevelen (VK) diagram, which shows H/C and O/C ratios for each formula in a
211 sample, can be used to describe the overall composition or evolution of organic mixtures
212 (Van Krevelen, 1993; Nizkorodov et al., 2011). Figure 3a shows a VK diagram for a
213 representative sample collected on 4 September 2011. It can be clearly seen from Figure 3a
214 that the majority of the CHO molecules in these samples have $O/C < 0.5$ and a large range of
215 H/C (0.5-2.0). While molecules with high H/C ratios (≥ 1.5) and low O/C ratios (≤ 0.5) (area A
216 in Fig. 4) are generally associated with aliphatic compounds, molecules with H/C ratios
217 (≤ 1.0) and O/C ratios (≤ 0.5) (area B in Fig. 3) typically belong to oxidised aromatic
218 hydrocarbons (Mazzoleni et al., 2012). In addition to oxidised aromatic hydrocarbons, the

219 low O/C and H/C cluster (area B) include a number N and S containing molecules. Such
220 prevalence in the aerosol samples from Cork suggests very strong anthropogenic influence at
221 the sampling site. In contrast, only a few ions were present in the aromatic region in aerosol
222 from the pristine boreal forest site Hyytiälä, Finland (Fig. 3b) (Kourtchev et al., 2013a).
223 Moreover, all of the compounds in area B in the Hyytiälä sample correspond to CHON
224 molecules. Although the sampling site at Cork is located only 400m from the shipping berth,
225 it is highly unlikely that the shipping emissions are responsible for the presence of a large
226 number of oxidised aromatic hydrocarbons. A previous study conducted at this site during
227 summer 2008 using an Aerosol Time-of-Flight (ATOF) MS indicated that shipping type
228 aerosol particles were observed in short, sharp events and contributed only 1.5% to ambient
229 PM_{2.5} mass (Healy et al., 2010). On the other hand, the same study suggested that vehicular
230 traffic is the largest source of ambient PM_{2.5} mass in Cork Harbour during summer time. The
231 presence of a very large number of species with high double bond equivalents (DBE) (≥ 6)
232 (Fig. 4), which shows the degree of unsaturation of a molecule, supports the inferences
233 derived from the Van Krevelen diagram (Fig. 3). It is worth mentioning that the compounds
234 associated with high DBE were not observed in the pristine boreal aerosol at Hyytiälä
235 associated with the clean Atlantic air masses (Fig 4, black circles) (Kourtchev et al., 2013a).
236 Molecular formulae with elemental ratios reflective of SOA (Wozniak et al., 2008) (area C,
237 Figure 3a and b) were present in most of the samples. Their contribution to the total number
238 of formulae was found to be the highest during the days with the lowest wind speed (below 2
239 m s⁻¹, 3 September and 13-15 September) and can possibly be explained by a lower dilution
240 of the aerosol.

241

242 *Tracers for marine sources*

243 The molecular composition of the aerosol samples was examined using Kendrick
244 Mass (KM) analysis, which is used for the identification of homologous series of compounds
245 differing only by the number of a specific base unit (e.g., a CH₂, CHO, groups). Kendrick
246 mass of the CH₂ unit is calculated by re-normalising the exact IUPAC mass (14.01565) of
247 CH₂ to 14.00000. The Kendrick Mass Defect (KMD) is calculated from the difference
248 between the nominal mass of the molecule and the exact KM (Hughley et al., 2001).
249 Depending on the sampling day, 95 to 97% of all peaks belong to CH₂ ‘homologous’ series
250 with >2 members. Figure 5 shows a KMD plot for the sample from 3 September 2011 (that
251 has the highest influence from local emissions as indicated by the low wind speed) where
252 KMD is expressed as a function of nominal KM. In this graph, all compounds with the same

253 base formula but different number of CH₂ groups have the same KMD value and thus appear
254 on a horizontal line. Therefore, the identification of molecular composition of one compound
255 in the homologous series allows elucidation of the remaining peaks in the series (Nizkorodov
256 et al., 2011). Considering the chemical complexity of the aerosol samples, the identification
257 of all series would be very impractical and speculative; therefore, in this study we
258 concentrated on the series that exhibited temporal variations or contained ions with very high
259 relative intensities (R.A >50%). Although due to competitive ionisation in the ESI direct
260 infusion analysis of the aerosol samples with a complex matrix the ion intensities do not
261 directly reflect the concentration of the molecules in the sample, it has been suggested that
262 semi-qualitative information on the relative concentrations between samples can still be
263 obtained (O'Brien et al., 2013). The distinguishably largest homologous series present in the
264 samples begins with a KM of 101.9541 corresponding to C₅H₁₀O₂, and is possibly associated
265 with a short chain unsaturated acid. This series included lauric acid (as identified by MS²
266 analysis), which exhibited very high ion intensity (up to 60% R.A.) during most of the
267 sampling period. Fatty acids, including lauric acid, can have multiple sources, which include
268 marine biota (e.g., Tervahattu et al., 2002), plant waxes (e.g., Simoneit et al., 1988), and
269 combustion of biomass material (e.g., Oros and Simoneit, 2001). The carbon number
270 prevalence (even or odd) of the fatty acids is often used for aerosol source identification.
271 During the sampling period, fatty acids exhibited strong even carbon number prevalence,
272 which indicates the importance of marine sources but also included molecules with an odd
273 carbon chain indicating their mixed origin. The site is located next to the river Lee, Lough
274 Mahon and only 15 km from the Celtic Sea, where phytoplankton and algae are very
275 abundant. Phytoplankton and algae are known to be an important source of fatty acids (e.g.,
276 Jeffries, 1970). The annual phytoplankton bloom in the Celtic Sea typically occurs from April
277 to October (ICES, 2008), which coincides with the aerosol sampling period. Fatty acids can
278 be emitted directly to the air or the dissolved material can be transferred to the air via bubble
279 bursting processes in sea spray. In this respect, a fair amount of sea salt in ambient particles
280 at the Cork harbour have been reported previously (Healy et al., 2010).

281

282 *Biomass burning markers*

283 N and/or S containing molecules had shorter homologous series compared to those
284 associated with CHO species (Fig. 5). Similar observations were reported for urban aerosol
285 from Cambridge, UK (Rincón et al., 2012) and boreal forest aerosol Hyytiälä, Finland
286 (Kourtchev et al., 2013a). Rincón et al. (2012) suggested that atmospheric oxidation reactions

287 resulting in the incorporation of sulfur and nitrogen functional groups do not conserve
288 homologous series but rather lead to a wide range of possible reaction products. The longest
289 N containing series had 10 homologues beginning with C₆H₅NO₃. Based on the MS² analysis
290 this molecule was tentatively identified as nitrophenol. Although nitrophenols can originate
291 from various sources including decomposition of herbicides and insecticides and burning of
292 coal and wood (Shafer and Schonherr, 1985) in urban environments primary motor vehicle
293 emissions are believed to be their major source (e.g., Tremp et al., 1993). Nitrophenols (2-
294 nitrophenol and 4-nitrophenol) have been previously observed in aerosol from urban
295 locations e.g., Rome, Italy (Cecinato et al., 2005), Mainz, Germany (Zhang et al., 2010) and
296 were mainly attributed to traffic emissions.

297 Another nitrogen containing series that is worth reporting included molecules with the
298 following molecular formulae: C₆H₅NO₄, C₇H₇NO₄, C₈H₉NO₄, C₉H₁₁NO₄ and C₁₀H₁₃NO₄.
299 These species were tentatively identified as nitroaromatic compounds (NACs), e.g.,
300 nitrocatechols, nitrophenols, nitroguaiacols and nitrosalicylic acids. NACs have been recently
301 detected in aerosol samples from urban location, e.g., Ljubljana, Slovenia (Kitanovski et al.,
302 2012) and rural environments e.g., Saxony, Germany (Inuma et al., 2010), K-Pusztá,
303 Hungary (Claeys et al., 2012) and Hyytiälä, Finland (Kourtchev et al., 2013a) and were
304 mainly attributed to biomass burning sources. The R.A. of these species showed a very high
305 correlation between each other in all Cork samples (Fig. 6) supporting their common origin.
306 Although NACs were observed throughout the whole sampling period, the highest intensities
307 of these molecules (up to R.A. 50%) were observed during 3 September and 13-15
308 September, which coincided with the highest OC concentration, the lowest temperature and
309 the lowest wind speed. This trend was also apparent in the Principal Component Analysis
310 (PCA, for method details see SI), where NACs are found to be closely correlated to each
311 other, moderately correlated to OC and EC and anticorrelated with temperature and wind
312 speed (Fig. 7). A previous study of PM_{2.5} aerosol in Cork harbor reported that biomass
313 burning in particular, combustion of domestic solid fuel (DSF), i.e., peat, coal, wood and
314 smokeless coal, is a substantial source of OC and PM_{2.5} even during summer (Kourtchev et
315 al., 2011; Healy et al., 2010).

316 The study by Kourtchev et al., (2011) used anhydrosugars, i.e., levoglucosan,
317 mannosan, galactosan and 1,6-anhydro- β -D-glucofuranose as marker compounds to estimate
318 the contribution of DSF burning. These anhydrosugars, structural isomers with a molecular
319 formula C₆H₁₀O₅, were also observed in all examined samples at *m/z* 161.0456. Although, an
320 ion at *m/z* 161.0456 exhibited the highest intensity (R.A. 20-25%) during 3 September

321 (sample TQ1) and 13-15 September (TQ12), it is only moderately correlated with the NACs
322 as indicated in the bidimensional plane defined by the first two principal components of the
323 PCA (Fig. 7). Competitive ionisation or ion suppression due to the presence of other matrix
324 compounds could be a reason for these observations. Despite this, the fairly high abundance
325 of the ion corresponding to the anhydrosugars with molecular formula $C_6H_{10}O_5$ suggests that
326 DSF burning is a major source of aerosol in Cork harbor. Similarly to the NACs, the
327 anhydrosugars ($C_6H_{10}O_5$) were moderately correlated to OC and EC and anticorrelated with
328 temperature and wind speed (Fig. 7). In addition, the PCA clearly supports the unique
329 composition of the two samples from 3 and 13-15 September as they form a cluster separate
330 from all other samples.

331

332 *Anthropogenic aging of biogenic SOA*

333 Another very intensive ion (R.A. up to 85%) at m/z 294.0654 observed in almost all
334 samples corresponded to a species with molecular formula $C_{10}H_{17}NSO_7$. This molecule has
335 been previously identified as α -/ β -pinene related NOS MW295 (Surratt et al., 2009; Gómez-
336 González et al., 2011) and was observed in various sampling locations including a Belgian
337 forest site at Brasschaat that is severely impacted by urban pollution (Gómez-González et al.,
338 2011), rural background sites at Birkenes (Norway), Lille Valby (Denmark) and Vavihill
339 (Sweden) (Yttri et al., 2011) and Hyytiälä (Finland) (Yttri et al., 2011; Kourtchev et al,
340 2013a). The OS and NOS are generally formed through heterogenous reactions of BVOCs
341 involving acidic sulfur aerosol (Surratt et al., 2008), which is primarily derived from
342 anthropogenic sources and therefore reflect anthropogenic influences at the sampling site. In
343 general, N and S containing compounds have very high ionisation efficiencies, and thus the
344 high abundance of the corresponding ions in the samples could be explained not only by
345 relatively high concentration of the compound but also by their favorable ionisation. LC/MS
346 analyses confirmed that the NOS MW295 was one of the major species in the Cork harbor
347 samples. Depending on the sampling day the concentration of NOS MW295 as determined by
348 LC/MS varied between 0.06 and 2.08 $ng\ m^{-3}$ with its maximum concentration peaking at
349 night-time. These values are comparable to concentration ranges (0.6-3.6 $ng\ m^{-3}$) for $PM_{2.5}$
350 aerosol from a Belgian forest site (Gómez-González et al., 2011). The later study also
351 observed night-time concentration increase of the NOS MW295 and linked it to enhanced
352 gas-to-particle partitioning at the cooler night-time temperatures or formation through night-
353 time chemistry with NO_x . 3-methyl-1,2,3-butanetricarboxylic (3-MBTCA), another α - and β -
354 pinene oxidation product (Szmigieslki et al., 2007), was detected in all studied samples in the

355 concentration range 0.03-0.28 ng m⁻³. 3-MBTCA has been previously identified as an OH-
356 initiated oxidation product of pinonic acid and was proposed as a suitable tracer for the
357 chemical aging of biogenic secondary organic aerosol (SOA) by OH radicals (Müller et al.,
358 2012).

359 Considering that increased concentration of α - and β -pinene derived NOS MW 295 was
360 observed during the time when the wind speed was the lowest (≤ 2 m s⁻¹) we can suggest that
361 the BVOC precursor responsible for the formation of this compound was rapidly oxidised by
362 the anthropogenic oxidants (e.g., NO_x). This is also confirmed by a presence of 3-MBTCA
363 and absence of the first generation α - and β -pinene oxidation products (e.g., pinic acid and
364 pinonic acid) in the samples. However, the lower air dilution during the days with the lowest
365 wind speed could also be responsible for these observations.

366 Another important BVOC derived NOS MW297 with the molecular formula C₉H₁₅NO₈S was
367 detected in the Cork samples by both direct infusion UHRMS and LC/MS analyses. This
368 molecule was previously identified as a limonene oxidation product (Surratt et al., 2008) and
369 was detected in various rural background sites (Yttri et al., 2011). The observed
370 concentrations of limonene derived NOS (0.2 ng m⁻³) in Cork site was lower than those
371 reported previously for rural background sites (0.5-1.5 ng m⁻³) (Yttri et al., 2011). The
372 difference can be explained by the type of vegetation and the density of the limonene
373 emitting species in Cork.

374 Among the identified OS, the presence of C₅H₁₂SO₇ in the Cork samples is worth reporting as
375 it is considered to be a tracer for isoprene, which is an important BVOC emitted by terrestrial
376 vegetation. This tracer compound was previously identified as C₅ organosulphate MW 216
377 and was suggested to be derived from isoprene epoxydiol isomers (Surratt et al., 2010).

378 A complete list of OS and NOS detected by direct infusion nanoESI UHRMS in one sample
379 associated with local emissions is shown in the Table S2. Although the alternatively applied
380 LC/MS method was able to detect (above detection limit) only two OS and two NOS
381 compared to (22-119 formulae) and (9-89 formulae), respectively identified by the direct
382 infusion nanoESI UHRMS, it provides invaluable quantitative information on the
383 contribution of specific OS and NOS in the aerosol mass.

384

385 **Conclusions**

386 In this study we applied direct infusion nanoESI UHR-MS and LC/ESI-(Q-TOF) MS for the
387 analysis of the organic fraction of 14 summer PM_{2.5} samples from an urban location in Cork,
388 Ireland. Up to 850 elemental formulae were identified with direct infusion analysis. The most

389 predominant groups of identified compounds included molecules with CHO, CHON and
390 CHOS. The occurrence and abundance of ions corresponding to nitrogen containing species
391 (likely ON) exhibited very strong night-time prevalence suggesting importance of NO₃
392 chemistry at the site.

393 Van Krevelen and DBE distributions along with relatively low elemental O/C and H/C ratios
394 indicated the presence of a large number of oxidised (poly-)aromatic compounds in the
395 samples, suggesting that the site is strongly influenced by traffic emissions. The
396 distinguishable homologous series in the KMD diagram contained saturated and unsaturated
397 fatty acid characteristic for primary marine emissions. The longest nitrogen containing series
398 included NACs, e.g., nitrocatechols, nitrophenols, nitroguaiacols and nitrosalicylic acids
399 derived from burning of DSF material. Most of the biogenic secondary organic aerosol
400 (SOA) compounds were found to later-generation SOA components such as NOS and OS.
401 The absence of major ‘fresh’ biogenic SOA components, such as pinic and *cis*-pinonic acid,
402 which are precursors for some of the identified OS and NOS, suggests a strong influence of
403 anthropogenic pollutants such as NO_x and SO₂ at the site, which might have quickly further
404 oxidised these first-generation SOA components. This conclusion is supported by the
405 presence of 3-MBTCA, a tracer for the aged biogenic secondary SOA, which was present in
406 all samples.

407 The results of this work demonstrate that the studied site is a very complex environment
408 dominated by a variety of industrial and domestic activities. Primary and secondary natural
409 sources of organic aerosol mass were also identified and it was suggested that anthropogenic
410 gaseous oxidants efficiently and significantly affect the composition of biogenic SOA at this
411 location resulting in a large number of nitrogen- and sulfur-containing organic compounds.

412

413 **Acknowledgements**

414

415 Research at the University of Cambridge was supported by a Marie Curie Intra-European
416 fellowship (project # 254319) and the European Research Council (ERC starting grant
417 279405).

418

419 **References**

420 Birch, M.E., Cary, R.A., 1996. Elemental carbon-based method for monitoring occupational
421 exposure to particulate diesel exhaust. *Aerosol Science and Technology* 25, 221–241.

422 Cecinato, A., Di Palo, V., Pomata, D., Sciano, M.C.T., Possanzini, M., 2005. Measurement of
423 phase-distributed nitrophenols in Rome ambient air. *Chemosphere* 59, 679–683.

424 Chameides, W., Lindsay, R., Richardson, J., Kiang, C., 1988. The role of biogenic
425 hydrocarbons in urban photochemical smog: Atlanta as a case study. *Science* 241, 1473–
426 1475.

427 Claeys, M., Vermeylen, R., Yasmeeen, F., Gómez-González, Y., Chi, X., Maenhaut, W., 2012.
428 Chemical characterisation of humic-like substances from urban, rural and tropical biomass
429 burning environments using liquid chromatography with UV/vis photodiode array detection
430 and electrospray ionisation mass spectrometry. *Environmental Chemistry* 9, 273–284.

431 Day, D.A., Liu, S., Russell, L.M., Ziemann, P.J., 2010. Organonitrate group concentrations in
432 submicron particles with high nitrate and organic fractions in coastal southern California.
433 *Atmospheric Environment* 44, 1970–1979.

434 Goldstein, A.H., Galbally, I.E., 2007. Known and unexplored organic constituents in the
435 Earth's atmosphere. *Environmental Science and Technology* 41, 1514–1521.

436 Healy, R.M., Hellebust, S., Kourtchev, I., Allanic, A., O'Connor, I.P., Bell, J.M., Healy,
437 D.A., Sodeau, J.R., Wenger, J.C., 2010. Source apportionment of PM_{2.5} in Cork Harbour,
438 Ireland using a combination of single particle mass spectrometry and quantitative semi-
439 continuous measurements. *Atmospheric Chemistry and Physics* 10, 9593-9613.

440 ICES, 2008. Celtic Sea and West of Scotland. In: ICES, editor. Advice book 5. pp. 12.

441 Inuma, Y., Böge, O., Gräfe, R., Herrmann, H., 2010. Methylnitrocatechols: Atmospheric
442 tracer compounds for biomass burning secondary organic aerosols. *Environmental Science
443 and Technology* 44, 8453-8459.

444 Jeffries, H.P., 1970. Seasonal composition of temperate plankton communities: fatty acids.
445 *Limnology Oceanography* 15, 419-426.

446 Kanakidou, M., Seinfeld, J.H., Pandis, S.N., Barnes, I., Dentener, F.J., Facchini, M.C., Van
447 Dingenen, R., Ervens, B., Nenes, A., Nielsen, C.J., 2005. Organic aerosol and global climate
448 modelling: a review. *Atmospheric Chemistry and Physics* 5, 1053–1123.

449 Kitanovski, Z., Grgić, I., Vermeylen, R., Claeys, M., Maenhaut, W., 2012. Liquid
450 chromatography tandem mass spectrometry method for characterization of monoaromatic
451 nitro-compounds in atmospheric particulate matter. *Journal of Chromatography A* 1268, 35–
452 43.

453 Kourtchev, I., Hellebust, S., Bell, J.M., O'Connor, I.P., Healy, R.M., Allanic, A., Healy, D.,
454 Wenger, J.C., Sodeau, J.R., 2011. The use of polar organic compounds to estimate the
455 contribution of domestic solid fuel combustion and biogenic sources to ambient levels of
456 organic carbon and PM_{2.5} in Cork Harbour, Ireland. *Science of the Total Environment* 409,
457 2143-2155.

458 Kourtchev, I., Fuller, S., Aalto, J., Ruuskanen, T.M., McLeod, M.W., Maenhaut, W., Jones,
459 R., Kulmala, M., Kalberer, M., 2013a. Molecular composition of boreal forest aerosol from
460 Hyytiälä, Finland, using ultrahigh resolution mass spectrometry. *Environmental Science and
461 Technology* 47, 4069-4079.

462 Kourtchev, I., Fuller, S.J., Giorio, C., Healy, R.M., Wilson, E., O'Connor, I.P., Wenger, J.C.,
463 McLeod, M., Aalto, J., Ruuskanen, T.M., Maenhaut, W., Jones, R., Venables, D.S., Sodeau,
464 J.R., Kulmala, M., Kalberer, M., 2013b. Molecular composition of biogenic secondary
465 organic aerosols using ultrahigh resolution mass spectrometry: comparing laboratory and
466 field studies. *Atmospheric Chemistry and Physics Discussions* 13, 29593-29627.

467 Kundu, S., Fisseha, R., Putman, A.L., Rahn, T.A., Mazzoleni, L.R., 2012. High molecular
468 weight SOA formation during limonene ozonolysis: insights from ultrahigh-resolution FT-
469 ICR mass spectrometry characterization. *Atmospheric Chemistry and Physics* 12, 5523–5536.

470 Love, C., Effelsberg, U., Mordehai, A., 2006 A comparative study of ESI, nano ESI and
471 HPLC-Chip MS ion sources for optimum sensitivity and sample throughput. ASMS poster.

472 Mazzoleni, L.R., Saranjampour, P., Dalbec, M.M., Samburova, V., Hallar, A.G., Zielinska,
473 B., Lowenthal, D.H., Kohl, S., 2012. Identification of water-soluble organic carbon in non-
474 urban aerosols using ultrahigh-resolution FT-ICR mass spectrometry: organic anions.
475 *Environmental Chemistry* 9, 285–297.

476 Müller, L., Reinnig, M.-C., Naumann, K.H., Saathoff, H., Mentel, T.F., Donahue, N.M.,
477 Hoffmann, T., 2012. Formation of 3-methyl-1,2,3-butanetricarboxylic acid via gas phase
478 oxidation of pinonic acid – a mass spectrometric study of SOA aging. *Atmospheric*
479 *Chemistry and Physics* 12, 1483-1496.

480 Nguyen, T.B., Roach, P.J., Laskin, J., Laskin, A., Nizkorodov, S.A., 2011. Effect of humidity
481 on the composition of isoprene photooxidation secondary organic aerosol. *Atmospheric*
482 *Chemistry and Physics* 11, 6931-6944.

483 Nizkorodov, S.A., Laskin, J., Laskin, A., 2011. Molecular chemistry of organic aerosols
484 through the application of high resolution mass spectrometry. *Physical Chemistry Chemical*
485 *Physics* 13, 3612–3629.

486 O'Brien, R.E., Laskin, A., Laskin, J., Liu, S., Weber, R., Russell, L., Goldstein, A.H., 2013.
487 Molecular characterization of organic aerosol using nanospray desorption/electrospray
488 ionization mass spectrometry: CalNex 2010 field study. *Atmospheric Environment* 68, 265-
489 272.

490 Oros, D.R., Simoneit, B.R.T., 2001. Identification and emission factors of molecular tracers
491 in organic aerosols from biomass burning part 1. Temperate climate conifers. *Applied*
492 *Geochemistry* 16, 1513–1544.

493 Putman, A.L., Offenberg, J.H., Fisseha, R., Kundu, S., Rahn, T.A., Mazzoleni, L.R., 2012.
494 Ultrahigh-resolution FT-ICR mass spectrometry characterization of alpha-pinene ozonolysis
495 SOA. *Atmospheric Environment* 46, 164–172.

496 Rincón, A.G., Calvo, A.I., Dietzel, M., Kalberer, M., 2012. Seasonal differences of urban
497 organic aerosol composition – an ultra-high resolution mass spectrometry study.
498 *Environmental Chemistry* 9, 298-319.

499 Roberts, J.M., 1990. The atmospheric chemistry of organic nitrates. *Atmospheric*
500 *Environment Part A-General Topics* 24, 243-287.

501 Shafer, W.E., Schonherr, J., 1985. Accumulation and transport of phenol, 2-nitrophenol, and
502 4-nitrophenol in plant cuticles. *Ecotoxicology and Environmental Safety* 10, 239–252.

503 Simoneit, B.R.T., Cox, R.E., Standley, L.J., 1988. Organic-matter of the troposphere.4.
504 Lipids in harmattan aerosols of Nigeria. *Atmospheric Environment* 22, 983–1004.

505 Surratt, J.D., Gómez-González, Y., Chan, A.W.H., Vermeylen, R., Shahgholi, M.,
506 Kleindienst, T.E., Edney, E.O., Offenberg, J.H., Lewandowski, M., Jaoui, M., Maenhaut,
507 W., Claeys, M., Flagan, R.C., Seinfeld, J.H., 2008. Organosulfate formation in biogenic
508 secondary organic aerosol. *Journal of Physical Chemistry A* 112, 8345-8378.

509 Surratt, J.D., Chan, A.W.H., Eddingsaas, N.C., Chan, M.N., Loza, C.L., Kwan, A.J., Hersey,
510 S.P., Flagan, R.C., Wennberg, P.O., Seinfeld, J.H., 2010. Reactive intermediates revealed in

511 secondary organic aerosol formation from isoprene. *Proceedings of National Academy of*
512 *Sciences USA* 107, 6640–6645.

513 Szmigielski, R., Surratt, J.D., Gómez-González, Y., Van der Veken, P., Kourtchev, I.,
514 Vermeylen, R., Blockhuys, F., Jaoui, M., Kleindienst, T.E., Lewandowski, M., Offenberg,
515 J.H., Edney, E.O., Seinfeld, J.H., Maenhaut, W., Claeys, M., 2007. 3-methyl-1,2,3-
516 butanetricarboxylic acid: An atmospheric tracer for terpene secondary organic aerosol.
517 *Geophysical Research Letters* 34 L24811, doi:10.1029/2007GL03133.

518 Tervahattu, H., Juhanoja, J., Kupiainen, K., 2002. Identification of an organic coating on
519 marine aerosol particles by TOF-SIMS. *Journal of Geophysical Research* 107, 4319,
520 doi:10.1029/2001JD001403.

521 Tremp, J., Mattrel, P., Fingler, S., Giger, W., 1993. Phenols and nitrophenols as tropospheric
522 pollutants – emissions from automobile exhausts and phase-transfer in the atmosphere. *Water*
523 *Air Soil Pollution* 68, 113–123.

524 Van Krevelen, D.W., 1993. *Coal: Typology-Physics-Chemistry-Constitution*, Elsevier
525 Science, Amsterdam, The Netherlands.

526 Wozniak, A.S., Bauer, J. E., Sleighter, R.L., Dickhut, R.M., Hatcher, P.G., 2008. Molecular
527 characterization of aerosol-derived water soluble organic carbon using ultrahigh resolution
528 electrospray ionization Fourier transform ion cyclotron resonance mass spectrometry.
529 *Atmospheric Chemistry and Physics* 8, 5099-5111.

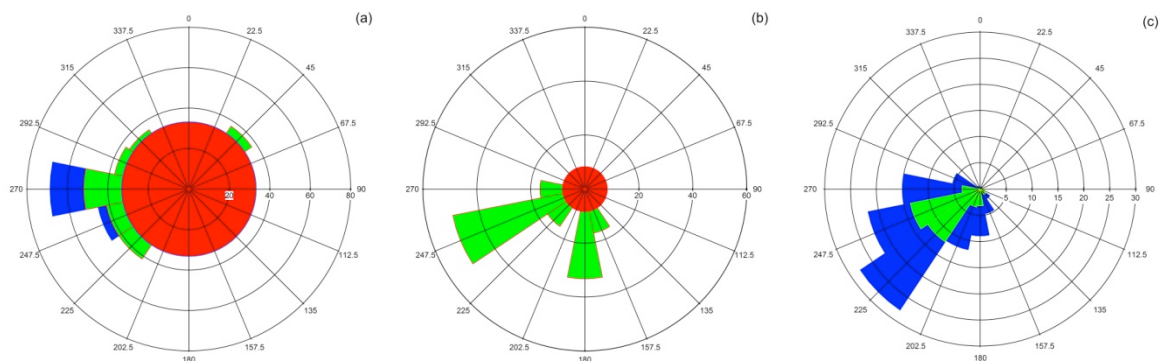
530 Yttri, K.E., Simpson, D., Nøjgaard, J.K., Kristensen, K., Genberg, J., Stenström, K.,
531 Swietlicki, E., Hillamo, R., Aurela, M., Bauer, H., Offenberg, J.H., Jaoui, M., Dye, C.,
532 Eckhardt, S., Burkhardt, J.F., Stohl, A., Glasius, M., 2011. Source apportionment of the
533 summer time carbonaceous aerosol at Nordic rural background sites. *Atmospheric*
534 *Chemistry and Physics* 11, 13339-13357.

535 Zhang, Y.Y., Müller, L., Winterhalter, R., Moortgat, G.K., Hoffmann, T., Pöschl, U., 2010.
536 Seasonal cycle and temperature dependence of pinene oxidation products, dicarboxylic acids
537 and nitrophenols in fine and coarse air particulate matter. *Atmospheric Chemistry and*
538 *Physics* 10, 7859-7873.

539

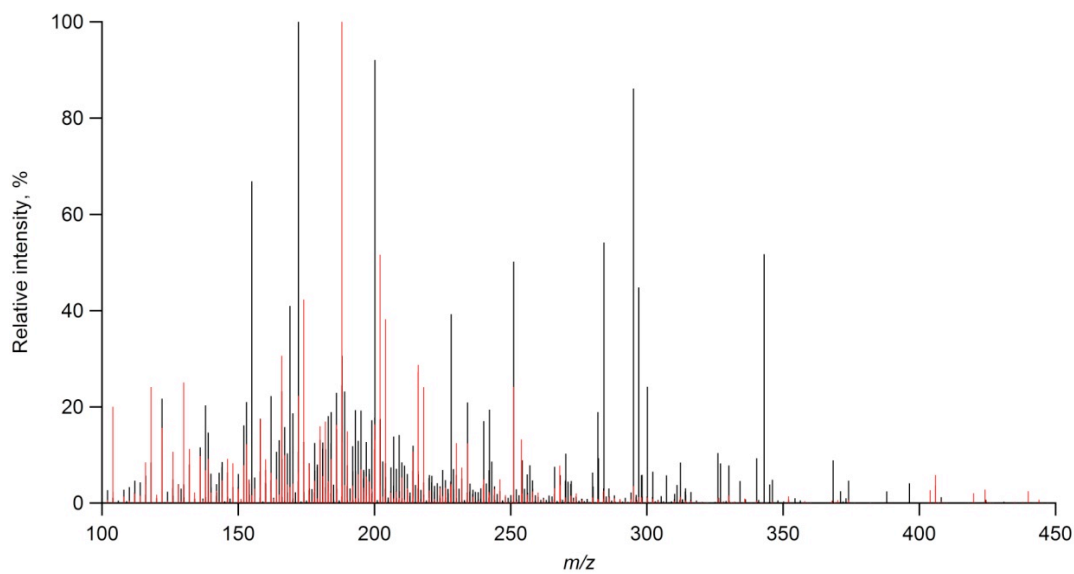
540

541 **Figures and captions:**



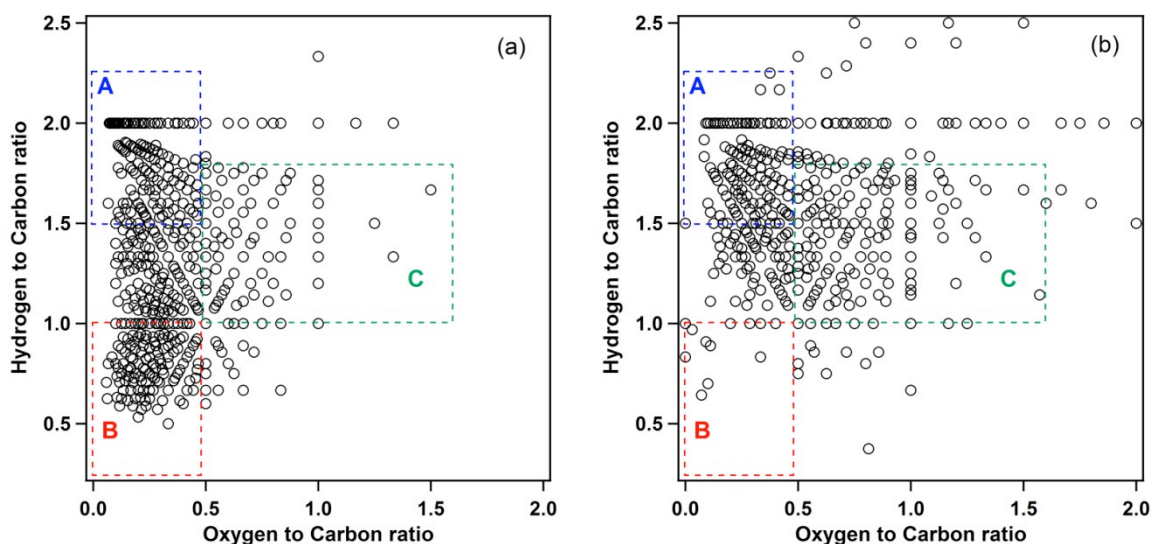
542

543 Figure 1. Wind roses for (a) 3 September, 2011; (b) 13-15 September, 2011 and (c) the rest of
544 the sampling period for 4-13 September and 15-19 September, 2011. The colour represent the
545 wind speed: blue $> 6 \text{ m s}^{-2}$ (strong wind); green $> 2 \text{ m s}^{-2}$ (light/gentle wind) and red $< 2 \text{ m s}^{-2}$
546 (calm wind conditions).



547

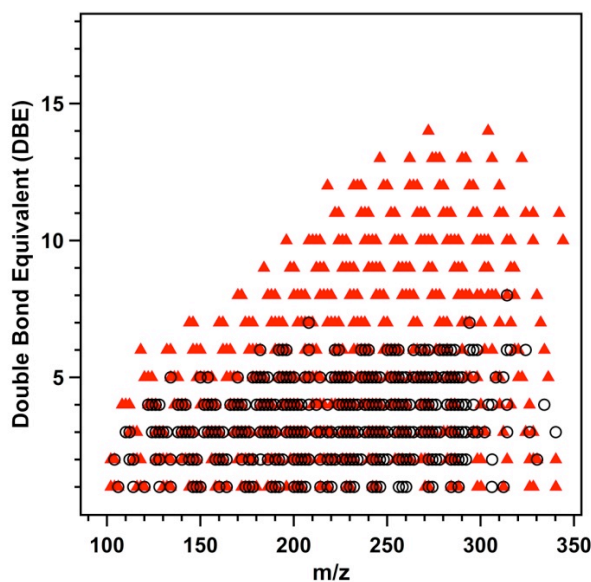
548 Figure 2. Direct infusion negative-nanoESI UHRMS blank corrected mass spectra obtained
549 for the representative day (in red) and night (in black) organic aerosol samples from Cork,
550 Ireland.



551

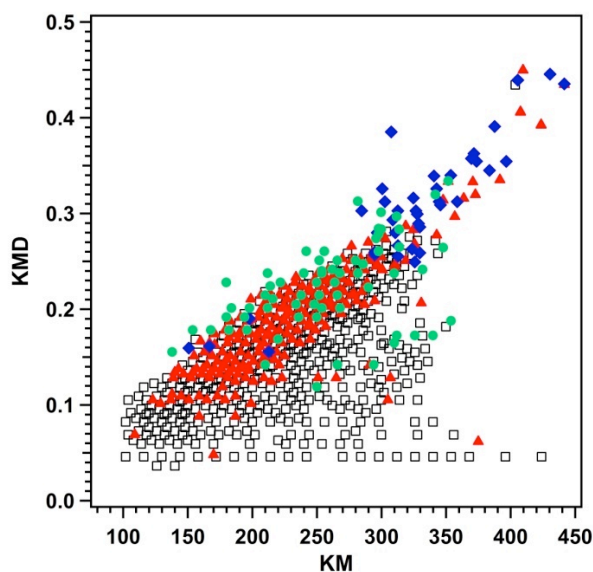
552 Figure 3. Van Krevelen (VK) diagrams for all detected ions in the aerosol samples from (a)
 553 an urban environment at Cork, Ireland, and (b) a remote boreal forest, Hyttiälä, Finland;
 554 Areas 'A', 'B' and 'C' indicate differences in the number of ions tentatively attributed to
 555 aliphatic, aromatic and secondary organic aerosol (SOA) species, respectively. All ions in
 556 the area 'B' of the boreal forest sample correspond to CHON molecules. The corresponding
 557 VK for the Hyttiälä's sample in Kourtchev et al. (2013a) only showed CHO and CHOS
 558 molecules.

559



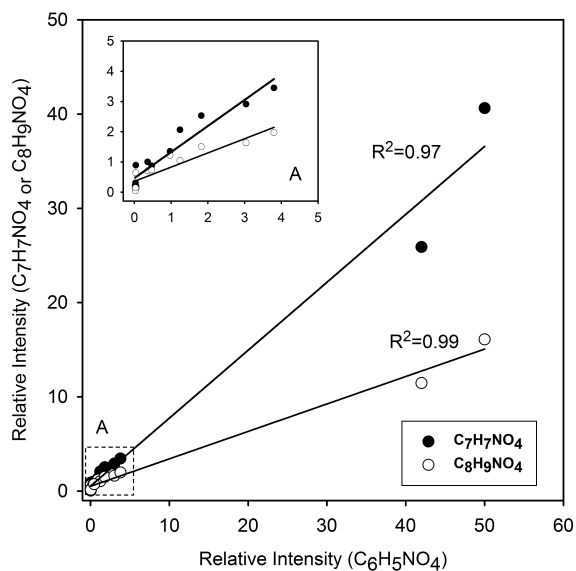
560

561 Figure 4. Double bond equivalents (DBE) vs. mass to charge ratio (m/z) for CHO molecules
 562 in the samples associated with local emissions from an urban site in Cork, Ireland collected
 563 on 3 September, 2011 (red triangles) and a boreal forest site at Hyttiälä, Finland, collected on
 564 17 August 2011 (black circles).



565

566 Figure 5. CH₂-Kendrick mass defect (KMD) vs. nominal Kendrick mass (KM) for CHO
 567 (black squares), CHON (red triangles), CHOS (green circles) and CHONS (blue diamonds)
 568 species in the aerosol sample from Cork, Ireland, associated with local emissions (from 3
 569 September, 2011).

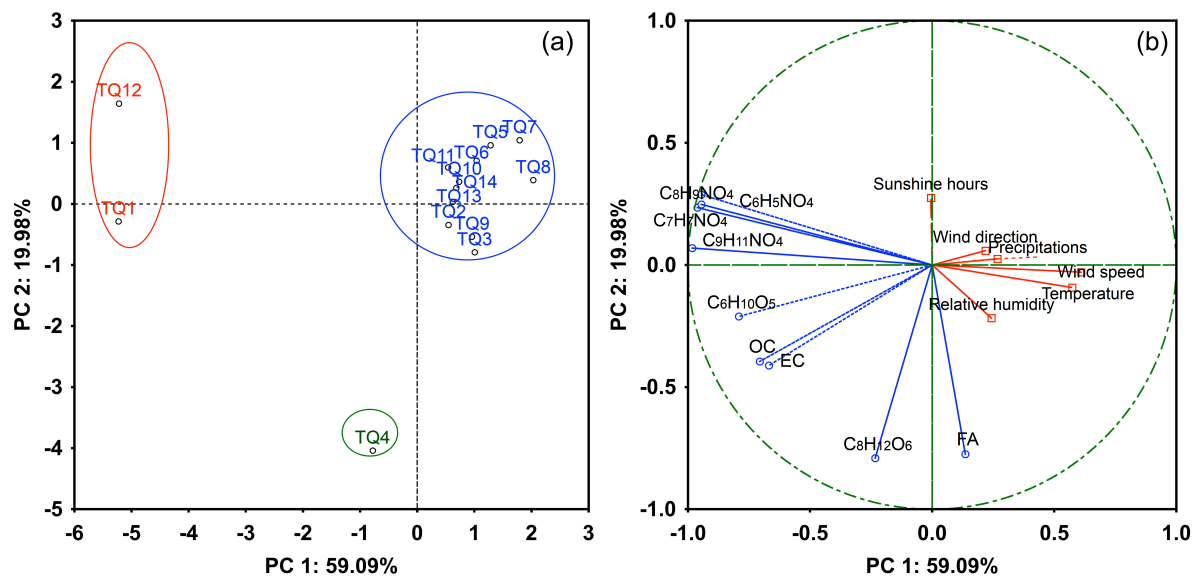


570

571 Figure 6. Correlation of relative intensities (RA) for nitroaromatic compounds (NACs) during
 572 the sampling period (3-17 September 2011) in Cork samples. The insert 'A' shows the strong
 573 correlation of these species even at low RA.

574

575



576

577 Figure 7. Scores (a) and loadings (b) of the first two principal components obtained from the
 578 principal components analysis and explaining the 79.07% of variance of the dataset. Red,
 579 blue and green ellipses show three distinct clusters in the scores plot (a). Vectors in blue and
 580 in red represent the active and supplementary variables in the loadings plot (b). Abbreviation
 581 FA corresponds to the ratio of even to odd carbon number of the detected fatty acids.

582

583